Cancer Cell
Article

A Prostatic Intraepithelial Neoplasia-Dependent $p27^{Kip1}$ Checkpoint Induces Senescence and Inhibits Cell Proliferation and Cancer Progression

Pradip K. Majumder,[1,2] Chiara Grisanzio,[3] Fionnuala O'Connell,[1,3] Marc Barry,[3] Joseph M. Brito,[1] Qing Xu,[1,2] Isil Guney,[1,2] Raanan Berger,[1,2] Paula Herman,[1,2] Rachel Bikoff,[1,2] Giuseppe Fedele,[1,3] Won-Ki Baek,[1,2] Shunyou Wang,[4] Katharine Ellwood-Yen,[4] Hong Wu,[4] Charles L. Sawyers,[5] Sabina Signoretti,[3] William C. Hahn,[1,2,6] Massimo Loda,[1,2,3,6,*] and William R. Sellers[1,2,7,*]

[1]Department of Medical Oncology, Dana-Farber Cancer Institute, Boston, MA 02115, USA
[2]Department of Medicine
[3]Department of Pathology
Brigham and Women's Hospital, Harvard Medical School, Boston, MA 02115, USA
[4]Department of Molecular and Medical Pharmacology, David Geffen School of Medicine, University of California, Los Angeles, Los Angeles, CA 90095, USA
[5]Human Oncology and Pathogenesis Program and Howard Hughes Medical Institute, Memorial Sloan-Kettering Cancer Center, New York, NY 10065, USA
[6]Broad Institute of MIT and Harvard, Cambridge, MA 02142, USA
[7]Novartis Institutes for BioMedical Research, Cambridge, MA 02139, USA
*Correspondence: massimo_loda@dfci.harvard.edu (M.L.), william.sellers@novartis.com (W.R.S.)
DOI 10.1016/j.ccr.2008.06.002

SUMMARY

Transgenic expression of activated *AKT1* in the murine prostate induces prostatic intraepithelial neoplasia (PIN) that does not progress to invasive prostate cancer (CaP). In luminal epithelial cells of Akt-driven PIN, we show the concomitant induction of $p27^{Kip1}$ and senescence. Genetic ablation of $p27^{Kip1}$ led to downregulation of senescence markers and progression to cancer. In humans, $p27^{Kip1}$ and senescence markers were elevated in PIN not associated with CaP but were decreased or absent, respectively, in cancer-associated PIN and in CaP. Importantly, $p27^{Kip1}$ upregulation in mouse and human in situ lesions did not depend upon mTOR or Akt activation but was instead specifically associated with alterations in cell polarity, architecture, and adhesion molecules. These data suggest that a $p27^{Kip1}$-driven checkpoint limits progression of PIN to CaP.

INTRODUCTION

Activation of AKT through deregulated phosphatidylinositol 3-kinase (PI3K) signaling resulting from genetic inactivation of phosphatase and tensin homolog (PTEN), mutational activation of PI3K, or the activation of upstream oncogenic tyrosine kinases is a frequent molecular event in human cancer (Brugge et al., 2007; Lee et al., 2007). We have previously shown that transgenic expression of activated Akt in the murine prostate induces a uniform and highly penetrant prostatic intraepithelial neoplasia (PIN) phenotype confined to the ventral prostate (Majumder et al., 2003). Even after long-term follow-up, these mice do not develop invasive cancers. However, in this model, there is robust and predictable time-dependent regression of the PIN with the mTOR inhibitor RAD001 (Majumder et al., 2004). This model thus provides a robust system in which to define transition steps leading from PIN to invasive cancer.

In human epithelial cancers, reduced levels of $p27^{Kip1}$ expression are frequently observed (Slingerland and Pagano, 2000) and are correlated with tumor progression and poor survival

SIGNIFICANCE

Most human epithelial cancers progress from dysplastic in situ lesions to invasive and ultimately metastatic disease. Prostatic intraepithelial neoplasia (PIN) is a precursor of invasive prostate cancer, but the molecular mechanisms underpinning this transition are largely unknown. Here we define loss of $p27^{Kip1}$ expression as a key event in this progression of PIN to invasive cancer. We further show that $p27^{Kip1}$ upregulation in PIN correlates with senescence in both murine and human prostate tissue. Upregulation of $p27^{Kip1}$ in preinvasive lesions is not dependent on mTOR or Akt activation but is secondary to loss of cell polarity and disruption of cell-cell adhesions. We suggest that the $p27^{Kip1}$-dependent checkpoint limits the progression of PIN to invasive cancer.

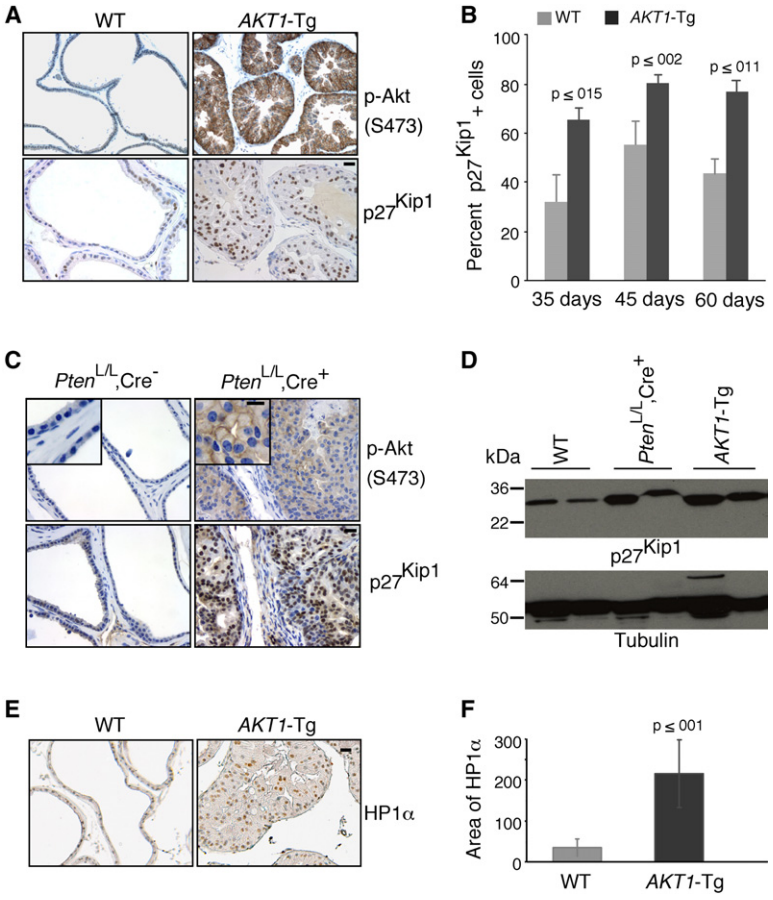

Figure 1. Induction of p27Kip1 and Senescence in Prostatic Intraepithelial Neoplasia of *AKT1*-Transgenic and *Pten*L/L;Cre+ Mice

(A) Ventral prostates (VPs) from wild-type (WT) and *AKT1*-transgenic (*AKT1*-Tg) mice were stained by immunohistochemistry using antibodies directed against phospho-Akt (S473) (upper panels) or p27Kip1 (lower panels). Scale bar = 50 μM.

(B) The number of cells staining positive for p27Kip1 was determined in VPs of WT and *AKT1*-Tg mice of the indicated ages. Data are presented as mean ± SEM.

(C) Wild-type (*Pten*L/L;Cre−) and *Pten* conditional knockout (prostate-specific) (*Pten*L/L;Cre+) VPs were stained with anti-phospho-Akt (S473) (upper panels) or anti-p27Kip1 (lower panels). Scale bar = 50 μM (100 μM in insert).

(D) Western blot analysis of p27Kip1 and tubulin in whole-cell lysates from VPs of WT, *Pten* conditional knockout (*Pten*L/L;Cre+), and *AKT1*-Tg mice at 6 weeks of age.

(E) VPs from WT and *AKT1*-Tg mice were stained with antibody against HP1α. Scale bar = 50 μM.

(F) The area of HP1α staining was measured in both WT and *AKT1*-Tg prostates. Data are presented as mean ± SD.

(Loda et al., 1997; Porter et al., 1997; Yang et al., 1998). p27Kip1 functions primarily as a negative regulator of cyclin-CDK activity and thus likely participates in tumor suppression by inhibiting cell-cycle progression (reviewed in Chu et al., 2008). Targeted disruption of p27Kip1 (*Cdkn1b*$^{-/-}$) in mice leads to prostatic hyperplasia (Cordon-Cardo et al., 1998) and development of pituitary adenomas (Fero et al., 1996, 1998) as the mice age. However, *Cdkn1b*$^{-/-}$ mice do not typically develop other spontaneous tumors (Fero et al., 1996; Kiyokawa et al., 1996; Nakayama et al., 1996).

In many human cancer cells, oncogene-induced senescence (OIS) is associated with known tumor suppressor pathways such as p53, VHL, and Rb (Serrano et al., 1997; Young et al., 2008). It has been reported that OIS occurs in many human and mouse precursors of cancer and that this phenomenon can be reversed by the inactivation of tumor suppressor pathways (Braig et al., 2005; Chen et al., 2005; Collado et al., 2005; Michaloglou et al., 2005). Recently, Young et al. (2008) have reported that senescence induced by loss of VHL in renal cancer cells is Rb, p27Kip1, and SKP2 dependent but p53 independent.

Here, we have investigated the role of p27Kip1 in tumor suppression in prostate cancer. Using both genetically engineered mice and human prostate samples, we have identified a relationship among senescence induction, p27Kip1 expression, and PIN that supports the notion that p27Kip1 induction in the context of early neoplastic lesions may represent a preinvasive checkpoint linked to cellular senescence.

RESULTS

p27Kip1 Protein and Markers for Cellular Senescence Are Increased in *AKT1*-Transgenic Prostate

Transgenic animals expressing activated Akt (*AKT1*-Tg) in the ventral prostate (VP) uniformly develop intraductal/intra-acinar lesions consistent with PIN. However, progression to invasive prostate cancer (CaP) has not been observed after 2 years of observation (data not shown). Moreover, despite the strong proliferative signal delivered by activated Akt in vitro, *AKT1*-Tg prostate shows only a modest increase in BrdU incorporation, suggesting a possible upregulation of cyclin-dependent kinase inhibitors (Majumder et al., 2004). Thus, to determine the level of p27Kip1 in the VP of *AKT1*-Tg mice, we performed immunohistochemical (IHC) analysis using anti-p27Kip1. While activation of Akt is associated with downregulation of p27Kip1 in a number of in vitro systems (Liang et al., 2002; Shin et al., 2002; Viglietto et al., 2002), surprisingly, p27Kip1 protein levels were significantly higher in prostate epithelial cells expressing Myr-*AKT1* when compared to littermate wild-type (WT) mice (Figures 1A and 1D). Similarly, significant levels of elevated p27Kip1 protein were observed in the VP of *AKT1*-Tg mice at 35, 45, and 60 days (Figure 1B).

We previously observed that PIN lesions in *AKT1*-Tg and *Pten* heterozygous (+/−) mice are histologically similar (Majumder et al., 2003). In the latter, activation of Akt is seen in conjunction with PTEN loss in PIN lesions (Majumder et al., 2003). Thus, we next examined mice harboring two floxed *Pten* alleles and a transgene driving the expression of prostate-restricted Cre (*ARR2PB*-Cre) (referred to as *Pten*L/L;Cre+) (Wang et al., 2003). We found that the development of PIN at 6 weeks of age was accompanied by phosphorylation and activation of Akt as well as a concomitant increase in p27Kip1 protein when compared to littermate controls (Figures 1C and 1D). These

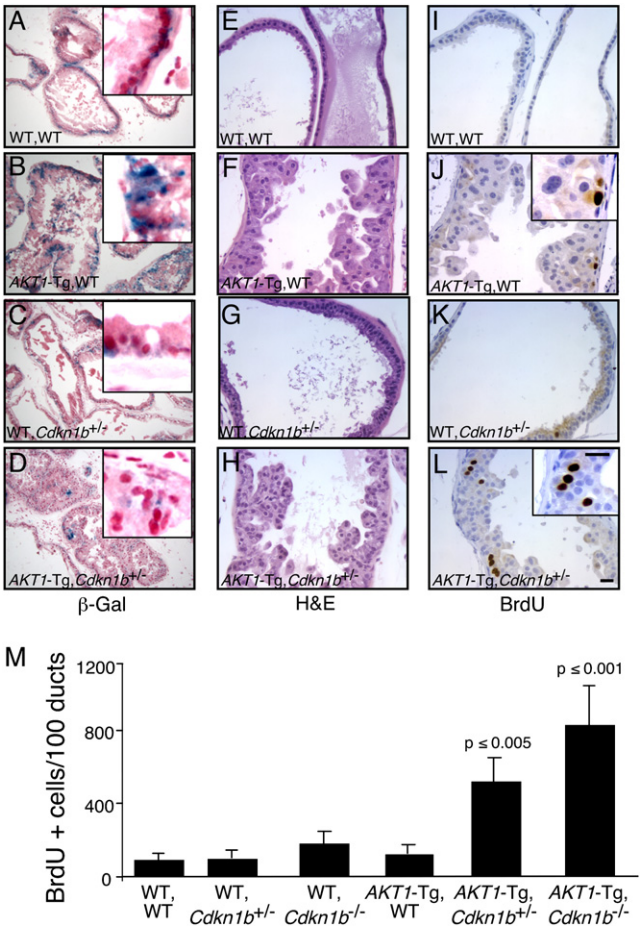

Figure 2. Genetic Inactivation of *Cdkn1b* Rescues Cells from Senescence and Increases Proliferation in *AKT1*-Transgenic Mice

(A–L) Twelve hours after BrdU administration, mice were sacrificed, and VPs of WT (A, E, and I), *AKT1*-Tg (B, F, and J), *Cdkn1b*$^{+/-}$ (C, G, and K), and *AKT1*-Tg/*Cdkn1b*$^{+/-}$ (D, H, and L) mice were stained with β-gal (A–D), hematoxylin and eosin (E–H), or anti-BrdU antibody (I–L). Scale bar = 50 μM (100 μM in insert).

(M) The number of BrdU-stained cells per 100 ducts was determined by manual counting of BrdU-positive cells in all VP lobes. Data are presented as mean ± SD.

data suggest that p27^{Kip1} is upregulated in the context of PIN driven either by myristoylation-dependent Akt activation or by loss of PTEN.

Cellular senescence is commonly seen in the early or precursor stages of invasive cancer (Braig et al., 2005; Chen et al., 2005; Collado et al., 2005; Michaloglou et al., 2005). To determine whether cells in the PIN lesions found in *AKT1*-Tg mice were senescent, we stained tissue sections for senescence-associated β-galactosidase (β-gal) in frozen tissue samples or for antibodies against HP1α and HP1γ in paraffin-embedded tissue (Bartkova et al., 2006). We found that the stabilization of p27^{Kip1} protein was associated with the increased levels of HP1α, HP1γ, and β-gal activity in the PIN lesions of the *AKT1*-Tg mice (Figures 1E and 1F; Figures 2A and 2B; data not shown).

Loss of p27^{Kip1} in *AKT1*-Tg Mice Rescues Cells from Senescence and Increases Proliferation in Prostate Epithelial Cells

It has been reported that oncogenes induce senescence in different human and murine precursors of cancer as well as in tumors harboring deletion of the *Pten* tumor suppressor (Braig et al., 2005; Chen et al., 2005; Collado et al., 2005; Michaloglou et al., 2005). Senescence induced by Pten deficiency has been reported to be dependent on p53. Inactivation of *Pten* causes cellular senescence, and combined inactivation of *Pten* and *p53* causes a lethal form of invasive prostate cancer (Chen et al., 2005). To test the hypothesis that the senescence observed in the PIN lesions of the *AKT1*-Tg mice could be reversed by the inactivation of the tumor suppressor p27^{Kip1}, compound mice were generated wherein Myr-*AKT1* was expressed in both the *Cdkn1b* heterozygous and homozygous null settings. PIN in the VP of *AKT1*-Tg mice displayed high β-gal activity (Figure 2B), and both HP1α and HP1γ were elevated (Figures 1D and 1E; data not shown). However, β-gal activity as well as expression of HP1α and HP1γ was decreased in the PIN lesions of mice in which *AKT1* was expressed in the context of the *Cdkn1b* heterozygous or homozygous background (Figures 2C and 2D; data not shown). These data suggest that the PIN-induced cellular senescence checkpoint is dependent on p27^{Kip1}.

These findings also raised the possibility that p27^{Kip1}-induced senescence results in a block in cell-cycle progression and consequently a failure to progress beyond the PIN phenotype. After administration of BrdU, VPs from 10- to 16-week-old offspring were harvested, and the rate of proliferation was determined by IHC detection of incorporated BrdU. Indeed, VPs from *AKT1*-Tg/*Cdkn1b*$^{+/-}$ and *AKT1*-Tg/*Cdkn1b*$^{-/-}$ mice showed significantly increased rates of BrdU incorporation (Figures 2L and 2M) as compared with *AKT1*-Tg/*Cdkn1b*$^{+/+}$, *AKT1*-WT/*Cdkn1b*$^{+/-}$, *AKT1*-WT/*Cdkn1b*$^{-/-}$, and *AKT1*-WT/*Cdkn1b*$^{+/+}$ prostates (Figures 2I–2K and 2M; data not shown). At 10–16 weeks of age, the PIN phenotype was exacerbated, but no additional cancer phenotype was observed at this time point (Figures 2E–2H). Thus, at early time points, loss of *Cdkn1b* abrogates the induction of senescence and results in increased prostate epithelial cell proliferation in the setting of Akt activation.

AKT1-Tg Mice Harboring Loss of Either One or Both *Cdkn1b* Alleles Develop Invasive Prostate Cancer

These observations were consistent with the notion that p27^{Kip1} acts as a checkpoint that limits hyperplastic proliferation and malignant transformation. To determine whether p27^{Kip1} loss also results in the progression from PIN to invasive CaP, we examined VPs of all genotypes resulting from the intercross of *AKT1*-Tg/*Cdkn1b*$^{+/-}$ mice as the mice aged. As predicted, *AKT1*-Tg/*Cdkn1b*$^{+/-}$ and *AKT1*-Tg/*Cdkn1b*$^{-/-}$ mice, but not littermate controls or *AKT1*-Tg/*Cdkn1b*$^{+/+}$ mice, developed invasive cancer in the VP (Figures 3A, 3B, and 3E; data not shown). Thirty-nine percent of *AKT1*-Tg/*Cdkn1b*$^{+/-}$ mice and 57% of *AKT1*-Tg/*Cdkn1b*$^{-/-}$ mice developed invasive CaP at the age of 1 year or more as compared with their control littermates (Figure 3E). One *AKT1*-Tg/*Cdkn1b*$^{+/-}$ and one *AKT1*-Tg/*Cdkn1b*$^{-/-}$ mouse developed a tumor in the VP prior to 1 year of age (Figure 3E; data not shown).

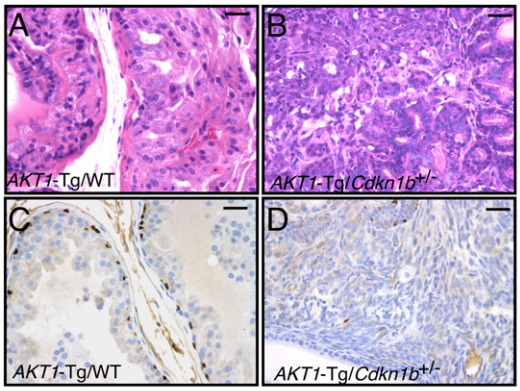

E

Age (wks)	WT, WT	*AKT1*-Tg, WT	WT, *Cdkn1b*$^{+/-}$	*AKT1*-Tg, *Cdkn1b*$^{+/-}$	WT, *Cdkn1b*$^{-/-}$	*AKT1*-Tg, *Cdkn1b*$^{-/-}$
⩽26	0/24	0/24	0/25	0/22	0/12	0/16
26-51	0/12	0/16	0/10	1/14	0/6	1/12
⩾52	0/18	1/30	0/14	14/36	0/6	8/14

Figure 3. Genetic Inactivation of *Cdkn1b* in *AKT1*-Transgenic Mice Results in Development of Invasive Prostate Cancer

(A) Prostatic intraepithelial neoplasia (PIN) in a representative section from the VP of an *AKT1*-Tg mouse (~52 weeks old). Scale bar = 100 μM.

(B) Invasive prostate cancer (CaP) in a representative section from an *AKT1*-Tg/*Cdkn1b*$^{+/-}$ mouse. Sections were stained with H&E. Scale bar = 100 μM.

(C) VP from an *AKT1*-Tg mouse stained with antibodies directed against p63. Scale bar = 100 μM.

(D) VP from an *AKT1*-Tg/*Cdkn1b*$^{+/-}$ mouse stained with antibodies directed against p63. Scale bar = 100 μM.

(E) Summary of tumor incidence by age and genotype.

Loss of the basal epithelial cell layer and hence loss of expression of the basal cell-specific marker p63 is a distinguishing feature of the transition from PIN (p63^{+}) to invasive CaP (p63^{-}) in humans (Signoretti et al., 2000). We therefore examined p63 expression in murine prostate tumors by IHC. While basal cells were present in the PIN lesions in VPs of *AKT1*-Tg mice (Figure 3C), prostate tumors from *AKT1*-Tg/*Cdkn1b*$^{+/-}$ and *AKT1*-Tg/*Cdkn1b*$^{-/-}$ mice (Figure 3D; data not shown) lacked the basal cell layer, confirming the invasiveness of these tumors. To further characterize the tumor phenotype, we examined the expression of the androgen receptor (AR) and the luminal cytokeratin 19 (CK19) by IHC and found that the tumors expressed readily detectable AR and CK19 (see Figures S1A and S1B available online; data not shown) but failed to express cytokeratin 14 and p63 (Figure 3D; data not shown). These observations demonstrate the luminal nature of these tumors, which is similar to human prostate cancer. Finally, BrdU incorporation assays showed that, as was the case in the PIN lesions arising in *AKT1*-Tg/*Cdkn1b*$^{+/-}$ and *AKT1*-Tg/*Cdkn1b*$^{-/-}$ mice, the resulting tumors were also highly proliferative (Figures S1C–S1F). IHC and immunoblot analysis of p27^{Kip1} suggested that these tumors retained the second allele of p27^{Kip1}, though protein levels were markedly reduced (Figures S2D–S2F and S2J). We noted that Akt expression was reduced in these tumors due to variegated expression of the transgene rather than to reduction of Akt on a per cell basis (data not shown).

Stabilization of p27^{Kip1} Is Dependent on the PIN Phenotype

The finding that p27^{Kip1} levels were increased in the *AKT1*-Tg mice raised the possibility that Akt activity might directly lead to elevated levels of p27^{Kip1}. Alternatively, p27^{Kip1} elevation might be associated with activation of the mTOR kinase or p70^{S6K} pathways further downstream of Akt. To distinguish among these possibilities, we took advantage of the mTOR dependence of this PIN phenotype. Specifically, inhibition of mTOR activity using the rapamycin derivative RAD001 (everolimus) leads to the resolution of the PIN phenotype by day 14 of treatment (Majumder et al., 2004). By comparing RAD001- and placebo-treated *AKT1*-Tg and wild-type mice, we hoped to distinguish the contribution of three possible effectors of p27^{Kip1} induction, namely the PIN phenotype itself (present or absent), mTOR (active or inactive), and Akt (active or inactive). To this end, 8- to 12-week-old *AKT1*-Tg and littermate wild-type mice were treated with placebo or RAD001 for 2 or 14 days. Consistent with our previous findings, 14 days after treatment, the VP histology of RAD001-treated *AKT1*-Tg mice reverted to normal (Figures 4A–4C; data not shown), while PIN persisted in placebo-treated *AKT1*-Tg mice (data not shown) and in mice treated with RAD001 for 2 days (Figure 4B).

We next examined p27^{Kip1} in the VP of *AKT1*-Tg mice treated with placebo or RAD001. Elevated levels of p27^{Kip1} were observed in the VP of *AKT1*-Tg mice treated with placebo (Figures 4P–4R) and *AKT1*-Tg mice treated with RAD001 for 2 days (Figures 4M and 4N). However, p27^{Kip1} levels reverted to normal after 14 days of treatment, concomitant with the disappearance of the PIN phenotype (Figures 4O and 4C). In *AKT1*-Tg animals, mTOR inhibition leads to the loss of phosphorylation of both eIF4G and S6 ribosomal protein (S6RP). In these experiments, S6RP phosphorylation was inhibited after 2 days of treatment with RAD001 (Figures 4H and 4I); however, p27^{Kip1} levels were unaffected (compare Figures 4M and 4N). As we had previously shown, the activation of Akt was unaffected by treatment with RAD001 and persisted on day 14, at which time both the PIN phenotype and the induction of p27^{Kip1} had resolved (Majumder et al., 2004; Figures 4D–4F). Thus, Akt oncogenic activity by itself is not sufficient for p27^{Kip1} induction (compare Figures 4F and 4O).

Finally, we have used expression profiling to identify two classes of transcripts indicative of either mTOR pathway activation (Majumder et al., 2004) or a distinct set of transcripts correlated with the presence or absence of the PIN phenotype. Aldolase 3 (a Hif-1 target) and prostate stem cell antigen (PSCA) are prototypical members of each class of transcripts, respectively. Consistent with the notion that p27^{Kip1} protein induction is linked to the PIN phenotype, elevated p27^{Kip1} levels correlated best with the pattern of mRNA induction seen with the phenotype marker PSCA and senescence markers rather than with the pharmacodynamic marker of mTOR activity aldolase 3 (Figure S3, upper panel). Together, these data, summarized in the lower panel of Figure S3, suggest that the cellular or morphological alterations secondarily arising during the formation of the PIN lesion either alone or together with activation of Akt lead to the induction of p27^{Kip1} followed by cellular senescence and a resulting block in both cell proliferation and phenotype progression.

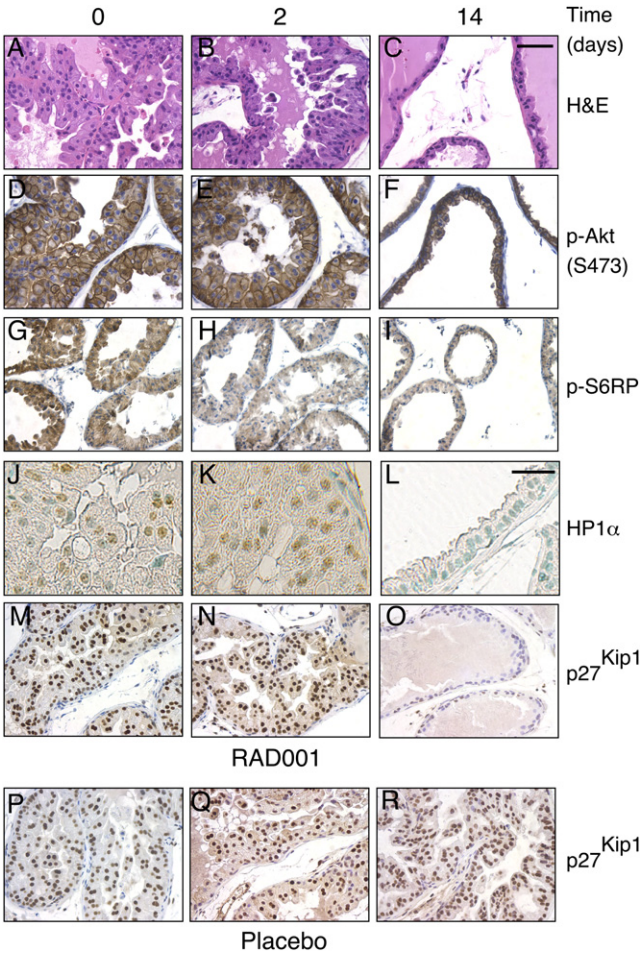

Figure 4. Induction of p27Kip1 and Increases in Senescence Markers Do Not Require mTOR Activation and Are Correlated with the PIN Phenotype

AKT1-Tg mice were treated orally with RAD001 at 10 mg/kg per day (A–O) or with placebo (P–R) for 0, 2, and 14 days. Shown are sections representative of results obtained in at least 12 animals evaluated after each specific treatment period. Scale bar = 100 μM in (A)–(I) and (M)–(R); scale bar = 200 μM in (J)–(L).

(A–C) Tissue sections from VPs stained with H&E.

(D–F) Tissue sections stained with antibody directed against phospho-Akt (S473).

(G–I) Tissue sections stained with antibody directed against phospho-S6RP.

(J–L) Immunohistochemical analysis was performed in tissue sections with antibody against HP1α.

(M–R) Tissue sections stained with antibody directed against p27Kip1.

A prediction that follows from these findings is that this putative p27Kip1 checkpoint might be activated in PIN lesions that are induced independently of PI3K pathway activation. Indeed, we also found significant elevation of p27Kip1 in the PIN phenotype of VPs of c-*Myc*-transgenic (*Myc*-Tg) mice as compared to wild-type controls (Figures S4A and S4B). The *Myc*-Tg mice developed invasive CaP at the age of 12 months, and in these cancers, p27Kip1 appeared to be downregulated as reported in human CaP (Figures 5F and 5G; Figures S4A and S4B). Thus, the p27Kip1 checkpoint correlates best with the appearance of PIN lesions.

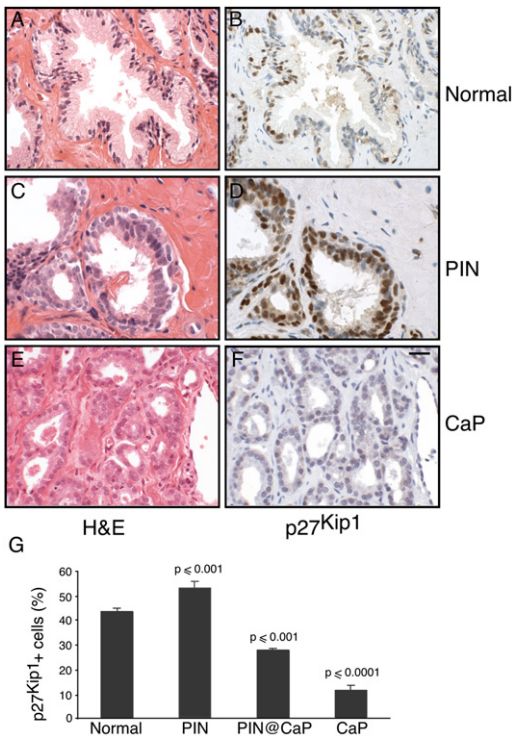

Figure 5. Stabilization of p27Kip1 in Human PIN

(A) Tissue section from normal human prostate stained with H&E.

(B) Normal prostate tissue section stained with antibody directed against p27Kip1.

(C) Tissue section from human PIN stained with H&E.

(D) PIN tissue section stained with antibody directed against p27Kip1.

(E) Tissue section from human prostate cancer (CaP) stained with H&E.

(F) CaP tissue section stained with antibody directed against p27Kip1. Scale bar = 50 μM in (A)–(F).

(G) The number of p27Kip1-positive cells was determined in normal tissue, PIN, PIN adjacent to CaP, and CaP. Data are presented as mean ± SEM.

The Relevance of p27Kip1 Elevation in Human PIN

Levels of p27Kip1 in representative foci of human benign prostatic epithelium, PIN, and invasive cancer were evaluated by IHC analysis. The level of p27Kip1 was significantly reduced in invasive cancer compared with benign epithelium (Figures 5D, 5F, and 5G), as reported previously (Guo et al., 1997; Thomas et al., 2000). Foci of PIN adjacent to invasive cancer consistently showed both a reduced intensity of staining and a reduced number of p27Kip1-positive cells compared with benign epithelium (Figure 5G; data not shown), as reported previously (De Marzo et al., 1998). In contrast, in 60% of the cases (15 of 25) of isolated PIN without adjacent invasive cancer, p27Kip1 staining was of similar intensity to adjacent benign epithelium (Figure 5B) and was present in a higher percentage of cells compared to benign epithelium (Figures 5D and 5G). The mean percentage of cells staining positively for p27Kip1 was 52.4% (range 38%–82%) in this subset of PIN and 42.9% (range 32%–50%) in the secretory cells of adjacent benign epithelium ($p < 0.001$) (Figure 5G). Thus, we confirmed that the increase in p27Kip1 in murine models of prostate cancer also occurs in primary human prostate cancers.

Human PIN Displays the Hallmark of Senescence

It has been reported that senescence is a hallmark of precursor lesions in many different human tumors (Braig et al., 2005; Chen et al., 2005; Collado et al., 2005; Michaloglou et al., 2005). In order to determine whether a senescence checkpoint could be identified in human PIN lesions, we performed pathological analysis of 21 frozen tissue samples from prostates with documented PIN. The PIN lesions were documented in 7 of the 21, and senescence was investigated by β-gal staining. Indeed, 4 of the 7 identified PIN lesions showed considerably more β-gal activity when compared to nondysplastic epithelial cells in the same tissue sections (Figures 6A and 6B). In addition, we characterized 44 human PIN lesions obtained from specimens without adjacent cancer, with normal counterparts from paraffin-embedded tissue sections. IHC and quantitative analysis by spectral imaging of HP1α and HP1γ showed increased levels of both markers in PIN lesions when compared to normal ducts (Figures 6C–6F; Figure S5D).

Induction of p27Kip1 during Detachment and Inhibition of Cell-Cell Contact in Human Primary Prostate Epithelial Cells

The PIN phenotype in *AKT1*-Tg mice is characterized by disorganization of luminal epithelial cells, including loss of appropriate cell polarization (see Majumder et al., 2004 and Figure 7A). In addition, in PIN lesions, numerous prostate epithelial cells are no longer in tight contact with the basement membrane or with nearby basal cells. These observations raised the possibility that epithelial cell detachment may trigger upregulation of p27Kip1 protein. To address this possibility, we turned to primary human prostate epithelial cells (PrECs) engineered to express SV40 large T antigen, the catalytic subunit of human telomerase (hTERT), and the AR (Berger et al., 2004; Garraway et al., 2003). These immortalized cells, PrEC-LEAR, were then transduced with a retrovirus encoding Myr-Akt to create PrEC-LEKAR cells. Next, these cells were plated on standard culture plates, on low-adhesion coated plates, or in suspension, and protein extracts were prepared after 24, 48, and 96 hr. In both cell lines, cell detachment led to a significant increase in p27Kip1 that was more notable in Akt-expressing cells (Figure 7C). These data support the notion that detachment of human prostate epithelial cells, either with or without Akt expression, leads to induction of p27Kip1. Similar results were also obtained in Rat1 fibroblasts transformed with Myr-*AKT1* (Figure 7B).

E-cadherin, a member of the cadherin family, mediates epithelial cell-cell interactions and maintains normal architecture and polarity of epithelial cells in tissue. It also plays an important role in the progression of many human cancers, including prostate cancer. We asked whether inhibition of cell-cell contact is sufficient to induce p27Kip1 stabilization in human primary prostate cancer cells. Suppression of E-cadherin expression in PrECs resulted in an inhibition of the normal architecture of cell-cell contact (Figure 7E) and increased the level of p27Kip1 protein (Figure 7D).

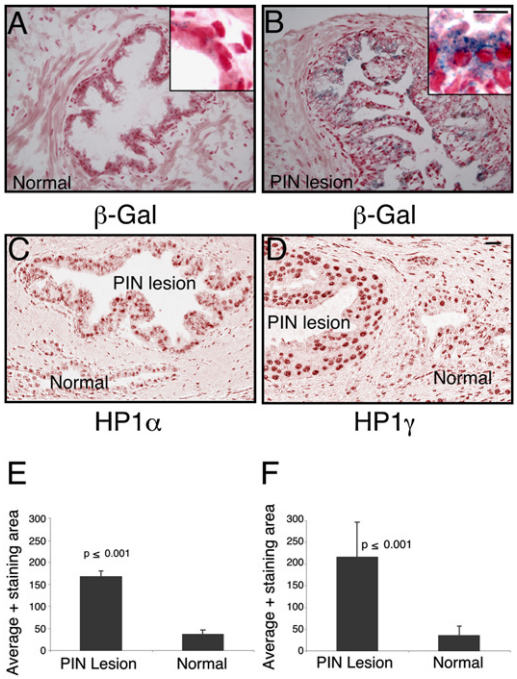

Figure 6. Markers of Cellular Senescence Are Elevated in Human PIN

(A and B) Frozen sections of normal human prostate (A) and PIN (B) were subjected to β-gal and H&E staining. Blue staining indicates β-gal activity; H&E was used as a counterstain to visualize the PIN lesion.

(C and D) Tissue sections from paraffin-embedded normal human prostate and PIN lesions were stained with antibodies against HP1α (C) and HP1γ (D). Scale bar = 50 μM in (A)–(D) (100 μM in insert).

(E and F) Average area of HP1α-positive (E) and HP1γ-positive (F) stain was measured in both PIN lesion and normal tissue. Data are presented as mean ± SD.

DISCUSSION

Cancer is characterized by a series of transitions from preneoplastic lesions to invasive cancer and finally metastatic disease. A great deal of emphasis has been placed on defining these events and understanding the disease progression at the molecular level in metastatic settings. However, less attention has been paid to the earlier transition points. It is not clear whether overcoming certain phenotypic transitions is only linked to checkpoints triggered by specific oncogenic mechanisms or whether such phenotypic transitions intrinsically raise specific checkpoint barriers that must be overcome. The angiogenic switch (as an example) or the epithelial-mesenchymal transition might represent such barriers or checkpoints to phenotypic transitions where tumors must acquire new properties in order to progress (Hanahan and Folkman, 1996).

We have studied the phenotypic transition between PIN and invasive cancer in a model of prostatic intraepithelial neoplasia resulting from transgenic activation of AKT. Here we show that in *AKT1*-transgenic and *Pten* homozygous mice, the PIN phenotype is associated with increased levels of p27Kip1 and the induction of markers of senescence. In order to determine whether the induction of p27Kip1 was causally related to the block in phenotype progression, we studied the results of genetic inactivation of *Cdkn1b* in the context of *AKT1*-Tg mice. Loss or downregulation of p27Kip1 led to increased proliferative rates, loss of senescence markers, and progression of the PIN phenotype to

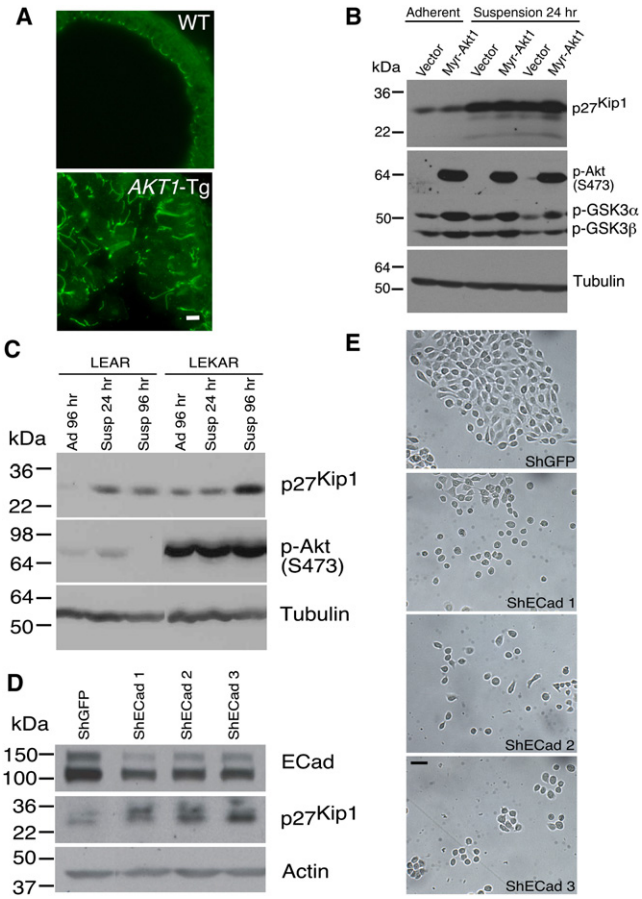

Figure 7. Disruption of Cellular Polarization and Adhesion Is Associated with Upregulation of p27Kip1 Level

(A) VPs of WT and *AKT1*-Tg mice stained with ZO-1 antibody and imaged by confocal microscope. Scale bar = 50 μM.

(B) Rat embryonic fibroblasts stably transfected with either vector or Myr-*AKT1* were cultured under adherent or suspension conditions. Protein lysates were prepared and immunoblotted with antibodies directed against p27Kip1 (upper panel), phospho-Akt (S473) and phospho-GSK3α and β (middle panel), and tubulin (lower panel).

(C) Protein lysates were prepared from primary human epithelial cells (LEAR and LEKAR) cultured under adherent (Ad) or suspension (Susp) conditions. Immunoblot analysis was performed using antibodies directed against p27Kip1 (upper panel), phospho-Akt (S473) (middle panel), and tubulin (lower panel).

(D) LEAR cells were transduced with three different shRNAs against E-cadherin and shGFP as a control. Cells were harvested 2 days postselection, and total protein lysates were prepared. Western blot analysis for E-cadherin (upper panel), p27Kip1 (middle panel), and actin (lower panel) was performed.

(E) LEAR cells transduced with E-cadherin shRNAs and shGFP control were grown in plates, and images were acquired 2 days postselection. Scale bar = 100 μM.

invasive cancer. These latter data are consistent with prior data showing that genetic inactivation of *Cdkn1b* in the context of *Pten*$^{+/-}$ mice produces an invasive cancer phenotype (Di Cristofano et al., 2001).

Cellular senescence opposes neoplastic transformation triggered by activation of oncogenic pathways both in vitro and in vivo (Chen et al., 2005; Collado et al., 2005). Inhibition of cellular proliferation in premalignant lesions in mouse and human might be the result of oncogene-induced senescence (Braig et al., 2005; Chen et al., 2005; Collado et al., 2005; Michaloglou et al., 2005). Chen et al. (2005) have shown that cells undergo senescence in preneoplastic lesions in Pten-deficient prostate. In addition, myristoylated Akt induces cellular senescence in primary murine embryonic fibroblasts (Miyauchi et al., 2004). These published data suggested that the senescence induced by loss of function of Pten is a result of Akt activation but requires p53. In contrast to these findings, more recent data demonstrate that cellular senescence due to the loss of another tumor suppressor gene, *VHL*, is p53 independent (Young et al., 2008). Thus, the cooperating events that contribute to the induction of senescence in preneoplastic lesions that occurs as a result of loss of a tumor suppressor gene or activation of an oncogene may be diverse.

In our model, we asked whether p27Kip1 and the senescence checkpoint are specifically associated with oncogene activation or with a phenotype-induced checkpoint. Careful dissection of the phenotype in response to mTOR inhibition coupled to measures of pathway activation for both Akt and mTOR demonstrated that increased p27Kip1 (Figures 4M–4O) and cellular senescence (Figures 4J–4L) are dependent on the preneoplastic lesions and do not depend directly upon either Akt or mTOR activation. Similarly, we did not find any correlation between mTOR activation and levels of p27Kip1 or senescence markers in a subset of clinical samples with PIN. However, correlation between loss of PTEN staining and activation of mTOR in these clinical PIN specimens was observed (Figure S5; data not shown). Thus, it appears that a PIN-dependent p27Kip1 checkpoint rather than an oncogene-induced checkpoint is enacted in the *AKT1*-Tg mice. Moreover, in *Myc*-Tg mice, p27Kip1 elevation was also seen in the PIN lesions. Thus, the checkpoint is apparently induced as a consequence of phenotypic perturbation that can be brought about by multiple upstream mechanisms. The apparent phenotype dependence of the p27Kip1 checkpoint may at least in part explain the synergy noted when *Cdkn1b* is genetically inactivated in the context of multiple other oncogenic or tumor suppressor manipulations and the high frequency of downregulation of p27Kip1 in human tumors.

It is not yet clear specifically what perturbation associated with the PIN phenotype might trigger accumulation of p27Kip1. Many possibilities, including loss of matrix association, loss of polarity, or loss of luminal-basal cell interactions, could be considered. Mammoto et al. (2004) previously found that restriction of extracellular matrix adhesion and inhibition of cell spreading are associated with induction of p27Kip1 and G1 arrest. In keeping with this notion, we found that in human prostate epithelial cells, p27Kip1 was induced under conditions of contact-free growth (Figures 7B and 7C). Recent data suggest that when E-cadherin is lost, cells fail to polarize (Capaldo and Macara, 2007). Here we showed that downregulation of E-cadherin expression by shRNA in primary human prostate cancer cells increased the level of p27Kip1 and disrupted cell-cell interactions (Figures 7D and 7E). We speculate that similar conditions might be recapitulated by loss of contact between epithelial cells and the basement membrane in vivo, as E-cadherin has been shown to be downregulated in human PIN as well as subsequent carcinoma (Jaggi et al., 2005). In addition, we have previously shown that PIN lesions in *AKT1*-Tg mice lose oriented zona occludens-1

localization and thus lose normal apical-basal cell polarity (Majumder et al., 2004). In fact, loss of polarity and detachment from basal cells and the basement membrane are characteristic of PIN. Links between the regulation of polarity and cell-cycle control are increasingly being recognized, particularly in tying cell orientation to oriented cell division (reviewed in Wodarz, 2001). Intriguingly, disruption of the polarized cytoskeleton and of bud formation in *Saccharomyces cerevisiae* is linked to delays in cell-cycle progression, dependent at least in part on Swe1, a CDK-inhibitory kinase (reviewed in Lew, 2003). Whether regulation of cell polarity is tied to a senescence checkpoint remains to be determined.

Importantly, these data are highly relevant to human prostate cancer. Indeed, we show that $p27^{Kip1}$ is overexpressed in human PIN not associated with invasive cancer, presumably representing the earliest phase of neoplastic transformation. In contrast, PIN adjacent to invasive cancer, where checkpoint loss may have already occurred, is associated with low levels of $p27^{Kip1}$. The role of $p27^{Kip1}$ in this process is further supported by a body of data showing that loss of $p27^{Kip1}$ is commonly found in human cancers (Chu et al., 2008) and that invasive tumor cells specifically degrade $p27^{Kip1}$. This in turn results in increased CDK2 activity (Loda et al., 1997).

As many as 30% of men with a diagnosis of PIN on biopsy are subsequently found to harbor an invasive prostatic adenocarcinoma on repeat biopsy (Gokden et al., 2005). Our findings therefore suggest that CDK inhibitors might have utility in preventing cancer progression from in situ dysplasia to invasion. Indeed, our group has previously shown that flavopiridol can in fact reduce the prevalence of esophageal cancer in a murine surgical model of Barrett's dysplasia and esophageal carcinoma in *Cdkn1b*$^{-/-}$ mice (Lechpammer et al., 2005). We have also demonstrated that preinvasive lesions of metaplastic esophageal mucosa in humans (Barrett's-associated dysplasias) also exhibit marked overexpression of $p27^{Kip1}$ with subsequent loss as invasion ensues, suggesting that upregulation of $p27^{Kip1}$ may be a checkpoint in other tissues as well (Singh et al., 1998). CDK inhibitors are in clinical trials for a number of human cancers. If safety and efficacy can be established, prevention trials with these agents in high-risk patients harboring preinvasive lesions could be considered.

EXPERIMENTAL PROCEDURES

Generation of Compound Heterozygous Mice

Cdkn1b heterozygous mice (B6.129S4-Cdkn1btm1Mlf/J), generated by the laboratory of James Roberts (Fred Hutchinson Cancer Research Center, Seattle), were obtained from the Jackson Laboratory (Fero et al., 1996). The heterozygous mice were bred to *AKT1*-Tg heterozygous mice (FVB-Tg/Pbsn-Akt1^{wrs9}) to generate F1 *AKT1*-Tg/*Cdkn1b* heterozygous mice. The compound *AKT1*-Tg heterozygous/*Cdkn1b* heterozygous mice were intercrossed to generate the F2 colony, and the resulting offspring were used in this study. All procedures were performed according to protocols approved by the Institutional Animal Care and Use Committee of the Dana-Farber Cancer Institute.

Genotyping, Dissections, and Preparation of Tissues

Isolation of genomic DNA from tail cuts or ear punches, PCR-based genotyping, prostate and genitourinary tract dissections, tissue fixation, and hematoxylin and eosin (H&E) stains were performed as described previously (Majumder et al., 2003; Xu et al., 2007). *Cdkn1b* heterozygous and homozygous mice were genotyped as described previously (Di Cristofano et al., 1998).

Administration of RAD001 or BrdU

40-O-(2-hydroxyethyl)-rapamycin (RAD001; 10 mg/kg/day) was administered as a microemulsion (Taesch and Niese, 1994) (2% w/w) diluted in double-distilled H_2O (ddH_2O) by oral gavage as described previously (Majumder et al., 2004). Mice receiving BrdU were injected intraperitoneally with 50 mg/kg of BrdU in PBS 12 hr prior to euthanasia and were sacrificed after immediate ventricular perfusion with 4% buffered formaldehyde.

Immunohistochemical and Immunoblot Analysis

Mounted tissue sections (both human and murine) were hydrated, incubated for 30 min with 3% H_2O_2 in methanol at room temperature, washed with ddH_2O and PBS, and heated in a microwave to 199°F in 1 mM EDTA (pH 8.0) for 25 min (for anti-$p27^{Kip1}$, anti-CK19, anti-phospho-Akt (S473), anti-phospho-S6RP, anti-AR, and anti-BrdU staining) or in 10 mM citrate buffer (pH 6.0) for 30 min (for anti-p63, anti-HP1α, and anti-HP1γ staining). Sections were blocked in 10% goat serum (Vector) for 30 min; incubated with anti-phospho-Akt (S473) (1:400), anti-phospho-S6RP (1:400), anti-AR (1:400) (Cell Signaling), anti-CK19 (1:200), anti-$p27^{Kip1}$ (1:200), anti-p63 (1:100), anti-BrdU (1:200) (BD PharMingen), anti-HP1α (1:1000) (clone 15.19s2, Upstate), or anti-HP1γ (1:1000) (clone 42s2, Upstate) in 1% BSA for 12 hr at 4°C; washed with PBS; and incubated with secondary antibody (1:200) (Vector Laboratories) for 30 min. Antigen-antibody complexes were detected with an ABC kit (Vector Laboratories) or by 3,3′-diaminobenzidine (DAB) followed by methyl green counterstaining (for HP1α and HP1γ). Frozen sections (5 μm thick) of VPs of different genotypes and frozen human prostate specimens were stained with β-gal (Calbiochem) and CK14. Protein extracts and immunoblots were prepared as described previously (Majumder et al., 2003). Anti-phospho-Akt (S473), anti-phospho-GSK3 (Cell Signaling), anti-$p27^{Kip1}$ (BD PharMingen), anti-E-cadherin (BD PharMingen), and anti-tubulin (B-5-1-2) (Sigma) were used at 1:1000.

Scoring of $p27^{Kip1}$ Immunohistochemistry in Human Prostate Specimens

Sixty-nine formalin-fixed cases of PIN were examined, including 44 cases of PIN with adjacent invasive CaP and 25 cases in patients without the histologic diagnosis of invasive cancer. All human tissues were collected from Brigham and Women's Hospital (Boston) using a protocol approved by the Partners Human Research Committee Institutional Review Board. Sections were stained with anti-$p27^{Kip1}$ antibody as described above. Three hundred cells from representative PIN foci, adjacent benign prostatic epithelium, and invasive cancer were counted, and the number of cells with nuclear $p27^{Kip1}$ staining was determined. Only cells in which the staining intensity was equal to or greater than the adjacent normal secretory prostatic epithelium were considered positive.

Twenty-one frozen human prostate biopsy tissues were stained with β-gal, and the presence of PIN was detected in seven samples. Higher levels of β-gal positivity compared to the adjacent normal cells were present in four of these seven.

Scoring of HP1α and HP1γ Staining in Mouse and Human Prostate Specimens

Both human (n = 44) and mouse (n = 20) prostate tissues were stained with anti-HP1α and HPγ. Since HP1 differential staining was low, localization and relative intensity were assessed using spectral imaging methods similar to those described previously (Byers et al., 2007). Spectral imaging and digital spectral cube deconvolution were performed using a CRi Nuance spectral analyzer (Cri, Inc.) and the associated software package. Image analysis and stain intensity quantitation were performed on the appropriate spectra using NIH ImageJ (http://rsb.info.nih.gov/ij/). Images were acquired at 20× objective magnification, and image intensities were normalized to a threshold value. Staining above the threshold intensity was considered positive, and the positive area within fields of 20 nuclei was measured.

Human Prostate Cell Lines, Rat Fibroblast Cells, and E-Cadherin Knockdown

Human primary prostate epithelial cells (PrECs) expressing SV40 large T antigen, *hTERT*, and AR without (PrEC-LEAR) or with myristoylated FLAG-*AKT1* (PrEC-LEKAR) (Berger et al., 2004) were plated on ultra-low attachment plates (Corning) at a density of 200,000 viable cells/ml in serum-free media (PrEGM)

as described previously (Berger et al., 2004). Spheres were collected by gentle centrifugation (800 rpm) after 1, 2, and 4 days and were dissociated by incubation for 10 min in 0.05% trypsin, 0.53 mM EDTA (Invitrogen). LEAR cells were infected with three independent shRNAs against E-cadherin (shECad1, 5′-CCAGTGAACAACGATGGCATT-3′; shECad2, 5′-CCAAGCAGAATTGCTCACATT-3′; and shECad3, 5′-CGATTCAAAGTGGGCACAGAT-3′) and control shGFP. Cells were harvested 2 days postselection. PrECs were lysed by sonication in 1.25% SDS, 0.0125 $NaPO_4$ (pH 7.2), 50 mM NaF, 2 mM EDTA, 1.25% NP-40, 1 mM sodium vanadate with protease inhibitors (Roche).

Rat embryonic fibroblast cells were infected with Myr-*AKT1*, and a stable cell line was established by single-cell dilution. Expression of Myr-Akt was determined by immunoblot analysis using an antibody against phospho-Akt (S473). These cells were grown either in adherent cell culture dishes or in suspension for 24 hr. Cells were lysed and protein was isolated as described previously (Majumder et al., 2003).

Statistical Analysis

One-way ANOVA was used to test for differences in cell proliferation and IHC scores between different genotypes.

SUPPLEMENTAL DATA

The Supplemental Data include five figures and can be found with this article online at http://www.cancercell.org/cgi/content/full/14/2/146/DC1/.

ACKNOWLEDGMENTS

We thank Erguen Sahin for the generous gift of mouse-specific CK19 antibody, Michelangelo Fiorentino for IHC analysis of $p27^{Kip1}$ and HP1 in human PIN, and Heidi Lane of the Novartis Institutes for Biomedical Research (Oncology, Basel, Switzerland) for RAD001. We also thank Nandita Bhattacharya, Yeonju Shim, and Jennifer Kum for excellent technical support. This work was supported by the Linda and Arthur Gelb Center for Translational Research, National Cancer Institute grants K01 CA94223 (W.C.H.) and PO1 CA89021 (W.R.S.), the Prostate Cancer Foundation (R.B., W.C.H., M.L., and W.R.S.), the Damon Runyon Cancer Research Foundation (W.R.S.), and a Career Development Award from the DF/HCC Prostate Cancer SPORE (P.K.M).

W.C.H., M.L., and W.R.S. receive research support from and are consultants for the Novartis Institutes for BioMedical Research. W.R.S. is an employee of the Novartis Institutes for BioMedical Research. P.K.M. and K.E.-Y. are employees of Merck Research Laboratories Boston.

Received: October 6, 2006
Revised: January 3, 2008
Accepted: June 6, 2008
Published: August 11, 2008

REFERENCES

Bartkova, J., Rezaei, N., Liontos, M., Karakaidos, P., Kletsas, D., Issaeva, N., Vassiliou, L.V., Kolettas, E., Niforou, K., Zoumpourlis, V.C., et al. (2006). Oncogene-induced senescence is part of the tumorigenesis barrier imposed by DNA damage checkpoints. Nature *444*, 633–637.

Berger, R., Febbo, P.G., Majumder, P.K., Zhao, J.J., Mukherjee, S., Signoretti, S., Campbell, K.T., Sellers, W.R., Roberts, T.M., Loda, M., et al. (2004). Androgen-induced differentiation and tumorigenicity of human prostate epithelial cells. Cancer Res. *64*, 8867–8875.

Braig, M., Lee, S., Loddenkemper, C., Rudolph, C., Peters, A.H., Schlegelberger, B., Stein, H., Dorken, B., Jenuwein, T., and Schmitt, C.A. (2005). Oncogene-induced senescence as an initial barrier in lymphoma development. Nature *436*, 660–665.

Brugge, J., Hung, M.C., and Mills, G.B. (2007). A new mutational AKTivation in the PI3K pathway. Cancer Cell *12*, 104–107.

Byers, R.J., Di Vizio, D., O'Connell, F., Tholouli, E., Levenson, R.M., Gossage, K., Twomey, D., Yang, Y., Benedettini, E., Rose, J., et al. (2007). Semiautomated multiplexed quantum dot-based in situ hybridization and spectral deconvolution. J. Mol. Diagn. *9*, 20–29.

Capaldo, C.T., and Macara, I.G. (2007). Depletion of E-cadherin disrupts establishment but not maintenance of cell junctions in Madin-Darby canine kidney epithelial cells. Mol. Biol. Cell *18*, 189–200.

Chen, Z., Trotman, L.C., Shaffer, D., Lin, H.K., Dotan, Z.A., Niki, M., Koutcher, J.A., Scher, H.I., Ludwig, T., Gerald, W., et al. (2005). Crucial role of p53-dependent cellular senescence in suppression of Pten-deficient tumorigenesis. Nature *436*, 725–730.

Chu, I.M., Hengst, L., and Slingerland, J.M. (2008). The Cdk inhibitor p27 in human cancer: prognostic potential and relevance to anticancer therapy. Nat. Rev. Cancer *8*, 253–267.

Collado, M., Gil, J., Efeyan, A., Guerra, C., Schuhmacher, A.J., Barradas, M., Benguria, A., Zaballos, A., Flores, J.M., Barbacid, M., et al. (2005). Tumour biology: senescence in premalignant tumours. Nature *436*, 642.

Cordon-Cardo, C., Koff, A., Drobnjak, M., Capodieci, P., Osman, I., Millard, S.S., Gaudin, P.B., Fazzari, M., Zhang, Z.F., Massague, J., and Scher, H.I. (1998). Distinct altered patterns of p27KIP1 gene expression in benign prostatic hyperplasia and prostatic carcinoma. J. Natl. Cancer Inst. *90*, 1284–1291.

De Marzo, A.M., Meeker, A.K., Epstein, J.I., and Coffey, D.S. (1998). Prostate stem cell compartments: expression of the cell cycle inhibitor p27Kip1 in normal, hyperplastic, and neoplastic cells. Am. J. Pathol. *153*, 911–919.

Di Cristofano, A., Pesce, B., Cordon-Cardo, C., and Pandolfi, P.P. (1998). Pten is essential for embryonic development and tumour suppression. Nat. Genet. *19*, 348–355.

Di Cristofano, A., De Acetis, M., Koff, A., Cordon-Cardo, C., and Pandolfi, P.P. (2001). Pten and p27KIP1 cooperate in prostate cancer tumor suppression in the mouse. Nat. Genet. *27*, 222–224.

Fero, M.L., Rivkin, M., Tasch, M., Porter, P., Carow, C.E., Firpo, E., Polyak, K., Tsai, L.H., Broudy, V., Perlmutter, R.M., et al. (1996). A syndrome of multiorgan hyperplasia with features of gigantism, tumorigenesis, and female sterility in p27(Kip1)-deficient mice. Cell *85*, 733–744.

Fero, M.L., Randel, E., Gurley, K.E., Roberts, J.M., and Kemp, C.J. (1998). The murine gene p27Kip1 is haplo-insufficient for tumour suppression. Nature *396*, 177–180.

Garraway, L.A., Lin, D., Signoretti, S., Waltregny, D., Dilks, J., Bhattacharya, N., and Loda, M. (2003). Intermediate basal cells of the prostate: in vitro and in vivo characterization. Prostate *55*, 206–218.

Gokden, N., Roehl, K.A., Catalona, W.J., and Humphrey, P.A. (2005). High-grade prostatic intraepithelial neoplasia in needle biopsy as risk factor for detection of adenocarcinoma: current level of risk in screening population. Urology *65*, 538–542.

Guo, Y., Sklar, G.N., Borkowski, A., and Kyprianou, N. (1997). Loss of the cyclin-dependent kinase inhibitor p27(Kip1) protein in human prostate cancer correlates with tumor grade. Clin. Cancer Res. *3*, 2269–2274.

Hanahan, D., and Folkman, J. (1996). Patterns and emerging mechanisms of the angiogenic switch during tumorigenesis. Cell *86*, 353–364.

Jaggi, M., Johansson, S.L., Baker, J.J., Smith, L.M., Galich, A., and Balaji, K.C. (2005). Aberrant expression of E-cadherin and beta-catenin in human prostate cancer. Urol. Oncol. *23*, 402–406.

Kiyokawa, H., Kineman, R.D., Manova-Todorova, K.O., Soares, V.C., Hoffman, E.S., Ono, M., Khanam, D., Hayday, A.C., Frohman, L.A., and Koff, A. (1996). Enhanced growth of mice lacking the cyclin-dependent kinase inhibitor function of p27(Kip1). Cell *85*, 721–732.

Lechpammer, M., Xu, X., Ellis, F.H., Bhattacharaya, N., Shapiro, G.I., and Loda, M. (2005). Flavopiridol reduces malignant transformation of the esophageal mucosa in p27 knockout mice. Oncogene *24*, 1683–1688.

Lee, J.Y., Engelman, J.A., and Cantley, L.C. (2007). Biochemistry. PI3K charges ahead. Science *317*, 206–207.

Lew, D.J. (2003). The morphogenesis checkpoint: how yeast cells watch their figures. Curr. Opin. Cell Biol. *15*, 648–653.

Liang, J., Zubovitz, J., Petrocelli, T., Kotchetkov, R., Connor, M.K., Han, K., Lee, J.H., Ciarallo, S., Catzavelos, C., Beniston, R., et al. (2002). PKB/Akt phosphorylates p27, impairs nuclear import of p27 and opposes p27-mediated G1 arrest. Nat. Med. *8*, 1153–1160.

Loda, M., Cukor, B., Tam, S.W., Lavin, P., Fiorentino, M., Draetta, G.F., Jessup, J.M., and Pagano, M. (1997). Increased proteasome-dependent degradation of the cyclin-dependent kinase inhibitor p27 in aggressive colorectal carcinomas. Nat. Med. *3*, 231–234.

Majumder, P.K., Yeh, J.J., George, D.J., Febbo, P.G., Kum, J., Xue, Q., Bikoff, R., Ma, H., Kantoff, P.W., Golub, T.R., et al. (2003). Prostate intraepithelial neoplasia induced by prostate restricted Akt activation: the MPAKT model. Proc. Natl. Acad. Sci. USA *100*, 7841–7846.

Majumder, P.K., Febbo, P.G., Bikoff, R., Berger, R., Xue, Q., McMahon, L.M., Manola, J., Brugarolas, J., McDonnell, T.J., Golub, T.R., et al. (2004). mTOR inhibition reverses Akt-dependent prostate intraepithelial neoplasia through regulation of apoptotic and HIF-1-dependent pathways. Nat. Med. *10*, 594–601.

Mammoto, A., Huang, S., Moore, K., Oh, P., and Ingber, D.E. (2004). Role of RhoA, mDia, and ROCK in cell shape-dependent control of the Skp2-p27kip1 pathway and the G1/S transition. J. Biol. Chem. *279*, 26323–26330.

Michaloglou, C., Vredeveld, L.C., Soengas, M.S., Denoyelle, C., Kuilman, T., van der Horst, C.M., Majoor, D.M., Shay, J.W., Mooi, W.J., and Peeper, D.S. (2005). BRAFE600-associated senescence-like cell cycle arrest of human naevi. Nature *436*, 720–724.

Miyauchi, H., Minamino, T., Tateno, K., Kunieda, T., Toko, H., and Komuro, I. (2004). Akt negatively regulates the in vitro lifespan of human endothelial cells via a p53/p21-dependent pathway. EMBO J. *23*, 212–220.

Nakayama, K., Ishida, N., Shirane, M., Inomata, A., Inoue, T., Shishido, N., Horii, I., and Loh, D.Y. (1996). Mice lacking p27(Kip1) display increased body size, multiple organ hyperplasia, retinal dysplasia, and pituitary tumors. Cell *85*, 707–720.

Porter, P.L., Malone, K.E., Heagerty, P.J., Alexander, G.M., Gatti, L.A., Firpo, E.J., Daling, J.R., and Roberts, J.M. (1997). Expression of cell-cycle regulators p27Kip1 and cyclin E, alone and in combination, correlate with survival in young breast cancer patients. Nat. Med. *3*, 222–225.

Serrano, M., Lin, A.W., McCurrach, M.E., Beach, D., and Lowe, S.W. (1997). Oncogenic ras provokes premature cell senescence associated with accumulation of p53 and p16INK4a. Cell *88*, 593–602.

Shin, I., Yakes, F.M., Rojo, F., Shin, N.Y., Bakin, A.V., Baselga, J., and Arteaga, C.L. (2002). PKB/Akt mediates cell-cycle progression by phosphorylation of p27(Kip1) at threonine 157 and modulation of its cellular localization. Nat. Med. *8*, 1145–1152.

Signoretti, S., Waltregny, D., Dilks, J., Isaac, B., Lin, D., Garraway, L., Yang, A., Montironi, R., McKeon, F., and Loda, M. (2000). p63 is a prostate basal cell marker and is required for prostate development. Am. J. Pathol. *157*, 1769–1775.

Singh, S.P., Lipman, J., Goldman, H., Ellis, F.H., Jr., Aizenman, L., Cangi, M.G., Signoretti, S., Chiaur, D.S., Pagano, M., and Loda, M. (1998). Loss or altered subcellular localization of p27 in Barrett's associated adenocarcinoma. Cancer Res. *58*, 1730–1735.

Slingerland, J., and Pagano, M. (2000). Regulation of the cdk inhibitor p27 and its deregulation in cancer. J. Cell. Physiol. *183*, 10–17.

Taesch, S., and Niese, D. (1994). Safety and tolerability of a new oral formulation of cyclosporin A, Sandimmun Neoral, in renal transplant patients. Transpl. Int. *7* (*Suppl 1*), S263–S266.

Thomas, G.V., Schrage, M.I., Rosenfelt, L., Kim, J.H., Salur, G., deKernion, J.B., Dorey, F., Said, J., and Reiter, R.E. (2000). Preoperative prostate needle biopsy p27 correlates with subsequent radical prostatectomy p27, Gleason grade and pathological stage. J. Urol. *164*, 1987–1991.

Viglietto, G., Motti, M.L., Bruni, P., Melillo, R.M., D'Alessio, A., Califano, D., Vinci, F., Chiappetta, G., Tsichlis, P., Bellacosa, A., et al. (2002). Cytoplasmic relocalization and inhibition of the cyclin-dependent kinase inhibitor p27(Kip1) by PKB/Akt-mediated phosphorylation in breast cancer. Nat. Med. *8*, 1136–1144.

Wang, S., Gao, J., Lei, Q., Rozengurt, N., Pritchard, C., Jiao, J., Thomas, G.V., Li, G., Roy-Burman, P., Nelson, P.S., et al. (2003). Prostate-specific deletion of the murine Pten tumor suppressor gene leads to metastatic prostate cancer. Cancer Cell *4*, 209–221.

Wodarz, A. (2001). Cell polarity: no need to reinvent the wheel. Curr. Biol. *11*, R975–R978.

Xu, Q., Majumder, P.K., Ross, K., Shim, Y., Golub, T.R., Loda, M., and Sellers, W.R. (2007). Identification of prostate cancer modifier pathways using parental strain expression mapping. Proc. Natl. Acad. Sci. USA *104*, 17771–17776.

Yang, R.M., Naitoh, J., Murphy, M., Wang, H.J., Phillipson, J., deKernion, J.B., Loda, M., and Reiter, R.E. (1998). Low p27 expression predicts poor disease-free survival in patients with prostate cancer. J. Urol. *159*, 941–945.

Young, A.P., Schlisio, S., Minamishima, Y.A., Zhang, Q., Li, L., Grisanzio, C., Signoretti, S., and Kaelin, W.G., Jr. (2008). VHL loss actuates a HIF-independent senescence programme mediated by Rb and p400. Nat. Cell Biol. *10*, 361–369.